THE CRASH PROGRAM - A SIMPLIFIED COLLISION RECONSTRUCTION PROGRAM

Raymond R. McHenry
Calspan Corporation

ABSTRACT

For several staged collisions, results obtained with a closed-form reconstruction calculation are compared with measured responses. The reconstruction procedure is defined, derivations of the analytical relationships are outlined and detailed results of sample applications are presented.*

INTRODUCTION

The analytical techniques that have traditionally been applied in reconstructions of highway accidents have predominently been "closed-form" calculations based on piecewise linear solutions of the equations of motion. The refinement of such approximation techniques has been hampered by the limited available response data from staged collisions and spinout trajectories. In the presently reported research, a refined closed-form calculation procedure has been developed through the use, in part, of time-history data generated with the Simulation Model of Automobile Collisions (SMAC) computer program (1-7).

*This paper is based on research performed under Contract Nos. DOT-HS-053-3-609 and DOT-HS-053-3-658 with the National Highway Traffic Safety Administration, U.S. Department of Transportation and Contract No. MVMA, CAL 7505-C4.11 with the Motor Vehicle Manufacturers Association. The contents of the paper reflect the views of the author, who is responsible for the facts and accuracy of the data presented herein, and do not necessarily reflect the official views or policy of the Department of Transportation or the Motor Vehicle Manufacturers Association.

The reported development has been aimed at achieving uniformity in the interpretation of physical evidence from automobile accidents. In particular, the speed change, ΔV, and its direction are believed to be the best indicators of exposure severity for the vehicle occupants. While the SMAC program has been demonstrated to yield reconstructed impact speed accuracies in the range of $\pm$ 5% its full benefits are achieved only with complete and accurate definitions of the scene evidence and it costs approximately $20 per run. The on-scene use of SMAC is strongly recommended in new investigations as a means of insuring completeness, compatibility and accuracy of the scene measurements. In relation to the overall costs of an investigation, the use of SMAC would involve a relatively small increase. In fact, the scene sketch and the reconstruction calculations and sketch produced by the on-scene SMAC system may more than offset the costs of corresponding off-scene efforts in reporting investigated cases.

In existing case reports, the frequently fragmentary reporting of scene data may not justify the costs of SMAC applications. Also, the large number of available case reports makes the cost per case for additional processing an important consideration. Therefore, the CRASH program, which has been demonstrated to yield $\pm$ 12% accuracy of speed estimates in reasonably well-documented cases at a computer cost of only approximately $5.00 per case, is believed to fill an existing need for a low cost accident reconstruction aid.

In the following, results obtained with the CRASH program are compared with experimental data for a number of collision configurations. The detailed analytical relationships that are used in the CRASH program are then presented and discussed.

COMPARISON OF RESULTS

Results of staged collisions that are suitable for use in evaluation of reconstruction techniques are relatively scarce. Many of the staged collisions for which at least partial response data are available include unrealistic effects from the viewpoint of reconstruction. For example, the extensively documented series of intersection-type collisions reported by

Severy, et al, in (13) involve the following unrealistic effects and/or data gaps.

(1) In many of the tests, full braking was applied abruptly, late in the spinout trajectories. However, the corresponding tire mark data are not reported and details of the brake applications in individual tests are not defined.

(2) The vehicles were towed toward the collision point with the transmissions in neutral. As a result, there was no engine braking during the spinouts.

(3) The tire-pavement friction coefficient was not measured.

(4) Damage dimensions are not reported.

(5) Speed-change data are not reported.

In car-to-car collisions staged by Calspan as a part of research in structural crashworthiness, the rest positions were not measured and the striking vehicle was "snubbed" subsequent to the impact by a trailing cable at a deceleration level substantially larger than that of full braking. Also, the struck vehicle was motionless at impact, making the collision conditions not representative of typical highway accidents.

As a result of the above difficulties with available measured response data, it has been necessary to use a "shotgun" approach in evaluating the validity of the developed techniques. Comparisons have been made with a large number of staged collisions, each of which has some shortcomings as a "standard", well-defined and representative accident. From a scientific viewpoint, this approach leaves much to be desired. It does not permit levels of confidence to be established in a rigorous manner. Rather, it merely indicates approximate error ranges in general applications. The results of nine sample applications are presented and discussed in the following paragraphs.

In some of the presented comparisons, the measured data have been supplemented with SMAC-generated damage or rest position data. Footnotes on the comparison tables define the use of such supplementary "evidence".

In relation to the comparisons, differences that exist in the analytical treatments of crush properties in the SMAC and CRASH programs should be noted. The SMAC program includes a coefficient of restitution based on data presented in (12) whereas the CRASH program uses a non-zero impact velocity intercept at zero residual crush to approximate the same effect. When actual damage dimensions are available, the error ranges of the two separate approximation techniques can be directly compared. However, in one of the presented comparisons for which damage information is not available, SMAC-generated damage data have been used as the basis for the CRASH approximation.

Offset Frontal (Table 1)

This experimental collision produced relatively large magnitudes of crush, and it is considered to be a good test of the damage analysis procedure within the CRASH program for an offset collision. However, the presence of sand around the impact point creates uncertainty regarding the effective tire-ground friction coefficient. The sand was applied to the surface in an attempt to reduce tire-terrain friction and to more clearly delineate tire mark evidence, since the vehicles were not braked and skid marks were expected to be minimal.

The value for ΔV that is listed under the SPIN II (Appendix 1) heading of CRASH is based primarily on the DAMAGE-generated value, as a result of the axial nature of the collision. The actual speed changes of the vehicles were not measured.

The CRASH reconstructions of the speeds at impact are considered to be reasonably close to the measured values, particularly in view of the uncertainty regarding the effective value of the tire-terrain friction coefficient.

Table 1

COLLISION CONFIGURATION: OFFSET FRONTAL

TEST IDENTIFICATION: CALSPAN MRA # 1

	MEASURED			CRASH		
				SPIN II		DAMAGE
	SPEED AT IMPACT	ΔV	VDI	SPEED AT IMPACT	ΔV	ΔV
	MPH	MPH		MPH	MPH	MPH
VEHICLE #1	30.5	-	12FYEW4	34.1 (+11.8%)	32.8	32.5
VEHICLE #2	31.5	-	12FYEW5	34.4 (+ 9.2%)	25.4	25.3

	REST POSITIONS			IMPACT POSITIONS			END OF ROTATIONAL AND/OR LAT. SKIDDING				ROLLING RESISTANCE				TIRE-PAVEMENT
	X'_{CR}	Y'_{CR}	ψ_R	X'_{CS}	Y'_{CS}	ψ_S	X'_{CI}	Y'_{CI}	ψ_I						
	FT.	FT.	DEG.	FT.	FT.	DEG.	FT.	FT.	DEG.	ROT.	RF	LF	RR	LR	μ
VEHICLE #1	-7.3	4.2	-25.0	-8.4	1.0	0.0	-	-	-	CCW	0.0	1.0	0.0	0.0	(0.5)
VEHICLE #2	0.7	-2.5	162.5	8.4	-1.0	180.0	-	-	-	CCW	0.0	1.0	0.0	0.0	(SAND)

	MEASURED DAMAGE DIMENSIONS										
	WIDTH	DAMAGE EXTENT				MOMENT ARM		DIRECTION			
	LI	CI1	CI2	CI3	CI4	DI	RATIO	ANGI	VEH. SIZE	VEH. WGT. LBS	REFERENCE
	IN.	IN.	IN.	IN.	IN.	IN.	RHOI	DEG.			
VEHICLE #1	34.0	46.5	(35.8)	(25.2)	14.5	-22.5	-	360°	3.	3080	2, 15
VEHICLE #2	35.0	57.0	(49.8)	(42.7)	35.5	-22.0	-	360°	3.	3950	

90° Rear-Side Impact at 40 MPH (Table 2)

In this case, the rest orientation of Vehicle #2 is not defined in (13) and had to be estimated. Because of the absence of VDIs and damage dimensions, SMAC-generated data were used for the damage analysis portion of CRASH. The tire-ground friction coefficient was estimated on the basis of SMAC and CRASH results for several of the individual tests in the series.

The CRASH reconstructions of speeds at impact are considered to be in excellent agreement with the measured values. While the actual speed changes of the vehicles were not measured, the two sets of estimates are in excellent agreement with each other. It is obvious that each aspect of the reconstruction technique is within range of being "tweaked" into agreement, via minor refinements, when improved experimental data are available.

Frontal, Head-On, Large Vs. Small (Table 3)

The fact that ΔV of each vehicle was measured in this experimental crash makes it of interest for the present comparison purposes. It was a relatively severe event, having a closing speed of approximately 88 miles per hour between a full-size and a compact vehicle.

The primary physical evidence consists of the damage dimensions and the vehicle weights. The striking vehicle was "snubbed" by a trailing cable subsequent to the collision, and the rest position of the struck vehicle was not measured. In the absence of rest position information, SMAC-generated data for rest and impact positions were used for the trajectory analysis portion of CRASH.

In view of the large extents of damage to the two vehicles and the fact that vehicles of different sizes were involved, the correlation of reconstruction results with experimental data is considered to be very good.

Table 2

COLLISION CONFIGURATION: 90° REAR-SIDE AT 40 MPH

TEST IDENTIFICATION: UCLA ITTE SIDE IMPACT SERIES

	MEASURED			CRASH		
				SPIN II		DAMAGE
	SPEED AT IMPACT	ΔV	VDI	SPEED AT IMPACT	ΔV	ΔV
	MPH	MPH		MPH	MPH	MPH
VEHICLE #1	40.0	-	-	37.3 (-6.8%)	14.7	14.9*
VEHICLE #2	40.0	-	-	39.6 (-1.0%)	14.7	14.9*

	REST POSITIONS			IMPACT POSITIONS			END OF ROTATIONAL AND/OR LAT. SKIDDING				ROLLING RESISTANCE				TIRE-PAVEMENT
	X'_{CR}	Y'_{CR}	ψ_R	X'_{CS}	Y'_{CS}	ψ_S	X'_{CI}	Y'_{CI}	ψ_I						
	FT.	FT.	DEG.	FT.	FT.	DEG.	FT.	FT.	DEG.	ROT.	RF	LF	RR	LR	μ
VEHICLE #1	50.0	-21.0	-147	-13.3	0.0	0.0	39.0	-20.0	-173	CCW	1.0	0.0	0.0	0.0	(0.8)
VEHICLE #2	19.8	-60.9	(-336)	0.0	-5.25	-90.0	-	-	-	CCW	0.0	0.0	1.0	1.0	

	MEASURED DAMAGE DIMENSIONS*										
	WIDTH	DAMAGE EXTENT				MOMENT ARM		DIRECTION			
	LI	CI1	CI2	CI3	CI4	DI	RATIO	ANGI	VEH. SIZE	VEH. WGT. LBS	REFERENCE
	IN.	IN.	IN.	IN.	IN.	IN.	RHOI	DEG.			
VEHICLE #1	(76.8)	(12.0)	(14.0)	(14.0)	(24.0)	(0.0)	-	-	3.	-	13, FIG. 7D
VEHICLE #2	(96.7)	(0.0)	(12.7)	(14.3)	(14.2)	(-71.2)	-	-	3.	-	

*SMAC-GENERATED DAMAGE DIMENSIONS USED IN CRASH

Table 3

COLLISION CONFIGURATION: FRONTAL, HEAD-ON, LARGE VS. SMALL

TEST IDENTIFICATION: CALSPAN TEST NO. 14

	MEASURED			CRASH		
				SPIN II		DAMAGE
	SPEED AT IMPACT	ΔV	VDI	SPEED AT IMPACT	ΔV	ΔV
	MPH	MPH		MPH	MPH	MPH
VEHICLE #1	43.8	63.8	12FDEW6	44.1* (+0.7%)	67.0 (+ 5.0%)	67.0 (+ 5.0%)
VEHICLE #2	43.8	26.3	12FDEW2	44.5* (+1.6%)	29.6 (+12.5%)	29.6 (+12.5%)

	REST POSITIONS *			IMPACT POSITIONS *			END OF ROTATIONAL AND/OR LAT. SKIDDING				ROLLING RESISTANCE				TIRE-PAVEMENT
	X'_{CR}	Y'_{CR}	ψ_R	X'_{CS}	Y'_{CS}	ψ_S	X'_{CI}	Y'_{CI}	ψ_I						
	FT.	FT.	DEG.	FT.	FT.	DEG.	FT.	FT.	DEG.	ROT.	RF	LF	RR	LR	μ
VEHICLE #1	(-51.9)	(0.0)	(-1.2)	(-8.0)	(0.0)	(0.0)	-	-	-	(CCW)	1.0	1.0	0.0	0.0	(0.8)
VEHICLE #2	(-12.6)	(0.0)	(180.6)	(5.9)	(0.0)	(180.0)	-	-	-	(CW)	1.0	1.0	0.0	0.0	

	MEASURED DAMAGE DIMENSIONS										
	WIDTH	DAMAGE EXTENT				MOMENT ARM		DIRECTION			
	LI	CI1	CI2	CI3	CI4	DI	RATIO	ANGI	VEH. SIZE	VEH. WGT. LBS	REFERENCE
	IN.	IN.	IN.	IN.	IN.	IN.	RHOI	DEG.			
VEHICLE #1	62.2	41.	41.	41.	41.	0.0	1.0	360°	1.	1750	14, 2
VEHICLE #2	62.2	23.	23.	23.	23.	0.0	1.0	360°	4.	3960	

*SMAC-GENERATED REST AND IMPACT DIMENSIONS.

Oblique Side Impact (Table 4)

The occurrence of two separate impacts makes this experimental crash of particular interest. The CRASH reconstruction of the speeds at impact for this case is considered to be in very good agreement with the measured values.

While the actual speed changes were not measured, the two sets of estimates are in reasonably good agreement with each other. The CRASH value for the speed change of Vehicle #1 reflects the underestimate of the impact speed of Vehicle #2. Since damage dimensions were not recorded, the damage analysis portion of CRASH made use only of vehicle weights, sizes and investigator-rated VDIs. Therefore, it is considered to be the least reliable of the sets of speed-change estimates. The reported values of ΔV are the vector sums of the results of two separate applications of CRASH for the two sets of VDIs.

Damage Analysis in Side Collisions (Tables 5, 6 and 7)

In Tables 5 and 6 results of CRASH applications to perpendicular side collisions, using damage dimensions and weights only, are presented. Note that the indicated maximum error of 15.7% in Table 5 corresponds to an actual discrepancy of only 1.1 MPH.

In Table 7 results of a CRASH application to an oblique, 45 degree angle, side collision are presented. In this case, only the Y component of the speed change of the struck vehicle was measured.

Trajectory Analysis in Intersection Collisions (Tables 8 and 9)

In Tables 8 and 9, results of CRASH applications to intersection-type collisions, using trajectory information only, are presented.

DAMAGE ANALYSIS

Hand calculation techniques for damage analysis that yield reasonable estimates of the impact velocity in frontal collisions (i.e., the relative velocity of approach) have been developed by Emori (full width contact only, (11)) and by Campbell (partial width contact, (9)), using linear approximations of the relationship between residual crush and impact velocity. The SMAC program (1-7) applies a similar analytical approach to the entire

Table 4

COLLISION CONFIGURATION OBLIQUE SIDE IMPACT

TEST IDENTIFICATION CALSPAN MRA # 3

	MEASURED			CRASH		
				SPIN II		DAMAGE
	SPEED AT IMPACT	ΔV	VDI	SPEED AT IMPACT	ΔV	ΔV
	MPH	MPH		MPH	MPH	MPH
VEHICLE #1	33.0	-	01RFEE2 02RZEW3	32.3 (-2.1%)	13.4	16.9*
VEHICLE #2	32.5	-	08LFEW3 08LZEW2	28.9 (-11.1%)	12.4	16.3*

	REST POSITIONS			IMPACT POSITIONS			END OF ROTATIONAL AND/OR LAT. SKIDDING				ROLLING RESISTANCE				TIRE-PAVEMENT
	X'_{CR}	Y'_{CR}	ψ_R	X'_{CS}	Y'_{CS}	ψ_S	X'_{CI}	Y'_{CI}	ψ_I						
	FT.	FT.	DEG.	FT.	FT.	DEG.	FT.	FT.	DEG.	ROT.	RF	LF	RR	LR	μ
VEHICLE #1	33.0	-17.0	-51.0	-0.5	-2.0	0.0	-	-	-	CCW	1.0	1.0	1.0	1.0	0.77
VEHICLE #2	43.0	-8.0	-39.0	6.5	7.5	-48.	-	-	-	CW	1.0	1.0	1.0	1.0	

	MEASURED DAMAGE DIMENSIONS										
	WIDTH	DAMAGE EXTENT				MOMENT ARM		DIRECTION			
	LI	CI1	CI2	CI3	CI4	DI	RATIO	ANGI	VEH. SIZE	VEH. WGT. LBS	REFERENCE
	IN.	IN.	IN.	IN.	IN.	IN.	RHOI	DEG.			
VEHICLE #1	-	-	-	-	-	-	-	-	3.	3095.	2
VEHICLE #2	-	-	-	-	-	-	-	-	3.	3338.	

*VECTOR SUM OF ΔV FROM TWO SEPARATE IMPACTS, BASED ON VDIs ONLY.

Table 5

COLLISION CONFIGURATION PERPENDICULAR SIDE COLLISION

TEST IDENTIFICATION CALSPAN TEST NO. 84

	MEASURED			CRASH: SPIN II		CRASH: DAMAGE
	SPEED AT IMPACT	ΔV	VDI	SPEED AT IMPACT	ΔV	ΔV
	MPH	MPH		MPH	MPH	MPH
VEHICLE #1	15.0	9.0	-	-	-	9.0 (0.0%)
VEHICLE #2	0.0	7.0	-	-	-	8.1 (+15.7%)

	REST POSITIONS			IMPACT POSITIONS			END OF ROTATIONAL AND/OR LAT. SKIDDING				ROLLING RESISTANCE				TIRE-PAVEMENT
	X'_{CR}	Y'_{CR}	ψ_R	X'_{CS}	Y'_{CS}	ψ_S	X'_{CI}	Y'_{CI}	ψ_I						
	FT.	FT.	DEG.	FT.	FT.	DEG.	FT.	FT.	DEG.	ROT.	RF	LF	RR	LR	μ
VEHICLE #1	-	-	-	-	-	-	-	-	-	-	-	-	-	-	-
VEHICLE #2	-	-	-	-	-	-	-	-	-	-	-	-	-	-	

	MEASURED DAMAGE DIMENSIONS										
	WIDTH	DAMAGE EXTENT				MOMENT ARM		DIRECTION			
	LI	CI1	CI2	CI3	CI4	DI	RATIO	ANGI	VEH. SIZE	VEH. WGT. LBS	REFERENCE
	IN.	IN.	IN.	IN.	IN.	IN.	RHOI	DEG.			
VEHICLE #1	79.2	1.5	(1.5)	(1.5)	1.5	0.0	1.0	0°	4.	3740.	16
VEHICLE #2	79.2*	3.7	(5.0)	(6.2)	7.5	10.0	-	90°	4.	4150.	

*Direct-contact damage only. Extent values scaled from Figure 3-3 of Reference 16.

Table 6

COLLISION CONFIGURATION: PERPENDICULAR SIDE COLLISION

TEST IDENTIFICATION: CALSPAN TEST NO. 85

	MEASURED			CRASH		
				SPIN II		DAMAGE
	SPEED AT IMPACT	ΔV	VDI	SPEED AT IMPACT	ΔV	ΔV
	MPH	MPH		MPH	MPH	MPH
VEHICLE #1	30.6	18.3	-	-	-	17.5 (-4.4%)
VEHICLE #2	0.0	16.0	-	-	-	16.2 (+1.3%)

	REST POSITIONS			IMPACT POSITIONS			END OF ROTATIONAL AND/OR LAT. SKIDDING				ROLLING RESISTANCE				TIRE-PAVEMENT
	X'_{CR}	Y'_{CR}	ψ_R	X'_{CS}	Y'_{CS}	ψ_S	X'_{CI}	Y'_{CI}	ψ_I						
	FT.	FT.	DEG.	FT.	FT.	DEG.	FT.	FT.	DEG.	ROT.	RF	LF	RR	LR	μ
VEHICLE #1	-	-	-	-	-	-	-	-	-	-	-	-	-	-	-
VEHICLE #2	-	-	-	-	-	-	-	-	-	-	-	-	-	-	

	MEASURED DAMAGE DIMENSIONS										
	WIDTH	DAMAGE EXTENT				MOMENT ARM		DIRECTION			
	LI	CI1	CI2	CI3	CI4	DI	RATIO	ANGI	VEH. SIZE	VEH. WGT. LBS	REFERENCE
	IN.	IN.	IN.	IN.	IN.	IN.	RHOI	DEG.			
VEHICLE #1	79.2	11.0	(12.0)	(13.0)	14.0	0.0	0.786	0^{o}	4.	3800	16
VEHICLE #2	79.2*	6.2	(8.9)	(11.6)	14.3	10.0	-	90^{o}	4.	4100	

*Direct-contact damage only. Extent values scaled from Figure 3-3 of Reference 16.

Table 7

COLLISION CONFIGURATION OBLIQUE SIDE COLLISION

TEST IDENTIFICATION CALSPAN TEST NO. 54

	MEASURED			CRASH		
				SPIN II		DAMAGE
	SPEED AT IMPACT	ΔV	VDI	SPEED AT IMPACT	ΔV	ΔV
	MPH	MPH		MPH	MPH	MPH
VEHICLE #1	45.7	23.1	12FREE3	-	-	20.8 (-10.0%)
VEHICLE #2	0.0	Y COMP. = 16.2	01RPEW3	-	-	19.4 Y COMP=14.9 (-8.0%)

	REST POSITIONS			IMPACT POSITIONS			END OF ROTATIONAL AND/OR LAT. SKIDDING				ROLLING RESISTANCE				TIRE-PAVEMENT
	X'_{CR}	Y'_{CR}	ψ_R	X'_{CS}	Y'_{CS}	ψ_S	X'_{CI}	Y'_{CI}	ψ_I						
	FT.	FT.	DEG.	FT.	FT.	DEG.	FT.	FT.	DEG.	ROT.	RF	LF	RR	LR	μ
VEHICLE #1	-	-	-	-	-	-	-	-	-	-	-	-	-	-	-
VEHICLE #2	-	-	-	-	-	-	-	-	-	-	-	-	-	-	

	MEASURED DAMAGE DIMENSIONS										
	WIDTH	DAMAGE EXTENT				MOMENT ARM		DIRECTION			
	LI	CI1	CI2	CI3	CI4	DI	RATIO	ANGI	VEH. SIZE	VEH. WGT. LBS	REFERENCE
	IN.	IN.	IN.	IN.	IN.	IN.	RHOI	DEG.			
VEHICLE #1	40.0*	0.0	(21.0)	(28.0)	28.0	19.0	0.250	5°	4.	3550	16
VEHICLE #2	96.0	0.0	12.0	16.8	0.0	0.0	-	50°	4.	3805.	

*Direct-contact damage only. Note that Appendix G of Reference 16 indicates 7 inches of crush at the left front corner. However, photographs and a supplementary data file indicate an induced elongation of 7 inches.

Table 8

COLLISION CONFIGURATION: 90° CENTER SIDE AT 40 MPH

TEST IDENTIFICATION: UCLA ITTE SIDE IMPACT SERIES

	MEASURED			CRASH: SPIN II		CRASH: DAMAGE
	SPEED AT IMPACT	ΔV	VDI	SPEED AT IMPACT	ΔV	ΔV
	MPH	MPH		MPH	MPH	MPH
VEHICLE #1	40.0	-	-	35.7 (-10.8%)	17.4	-
VEHICLE #2	40.0	-	-	37.3 (- 6.8%)	17.4	-

	REST POSITIONS			IMPACT POSITIONS			END OF ROTATIONAL AND/OR LAT. SKIDDING				ROLLING RESISTANCE				TIRE-PAVEMENT
	X'_{CR}	Y'_{CR}	ψ_R	X'_{CS}	Y'_{CS}	ψ_S	X'_{CI}	Y'_{CI}	ψ_I						
	FT.	FT.	DEG.	FT.	FT.	DEG.	FT.	FT.	DEG.	ROT.	RF	LF	RR	LR	μ
VEHICLE #1	30.0	-23.0	-250.0	-13.3	0.0	0.0	-	-	-	CCW	1.0	0.0	0.0	0.0	0.8
VEHICLE #2	23.7	-48.5	-316.0	0.0	0.0	-90.0	-	-	-	CCW	0.0	0.0	0.0	0.0	

	MEASURED DAMAGE DIMENSIONS										
	WIDTH	DAMAGE EXTENT				MOMENT ARM		DIRECTION			
	LI	CI1	CI2	CI3	CI4	DI	RATIO	ANGI	VEH. SIZE	VEH. WGT. LBS	REFERENCE
	IN.	IN.	IN.	IN.	IN.	IN.	RHOI	DEG.			
VEHICLE #1	-	-	-	-	-	-	-	-	3.	-	13
VEHICLE #2	-	-	-	-	-	-	-	-	3.	-	

Table 9

COLLISION CONFIGURATION: 90° REAR SIDE AT 30 MPH

TEST IDENTIFICATION: UCLA ITTE SIDE IMPACT SERIES

	MEASURED			CRASH		
				SPIN II		DAMAGE
	SPEED AT IMPACT	ΔV	VDI	SPEED AT IMPACT	ΔV	ΔV
	MPH	MPH		MPH	MPH	MPH
VEHICLE #1	30.0	-	-	31.3 (+4.3%)	10.2	-
VEHICLE #2	30.0	-	-	30.3 (+1.0%)	10.2	-

	REST POSITIONS			IMPACT POSITIONS			END OF ROTATIONAL AND/OR LAT. SKIDDING				ROLLING RESISTANCE				TIRE-PAVEMENT
	X'_{CR}	Y'_{CR}	ψ_R	X'_{CS}	Y'_{CS}	ψ_S	X'_{CI}	Y'_{CI}	ψ_I						
	FT.	FT.	DEG.	FT.	FT.	DEG.	FT.	FT.	DEG.	ROT.	RF	LF	RR	LR	μ
VEHICLE #1	43.1	-55.2	-55.0	-13.3	0.0	0.0	15.6	-9.0	-52.0	CCW	1.0	0.0	0.0	0.0	0.8
VEHICLE #2	12.9	-48.0	-347.0	0.0	-5.25	-90.0	-	-	-	CCW	0.0	0.0	0.0	0.0	

	MEASURED DAMAGE DIMENSIONS										
	WIDTH	DAMAGE EXTENT				MOMENT ARM		DIRECTION			
	LI	CI1	CI2	CI3	CI4	DI	RATIO	ANGI	VEH. SIZE	VEH. WGT. LBS	REFERENCE
	IN.	IN.	IN.	IN.	IN.	IN.	RHOI	DEG.			
VEHICLE #1	-	-	-	-	-	-	-	-	3.	-	13
VEHICLE #2	-	-	-	-	-	-	-	-	3.	-	

peripheral structure, and it has been demonstrated to yield good approximations of both impact velocity and speed change, ΔV, in general collision configurations including oblique, non-central impacts. The objective of the present research has been to develop a simple, closed-form damage analysis technique that is applicable to general collision configurations.

Central Collisions

In the case of central collisions (i.e., where the line-of-action of the collision force passes through the centers of masses of the two vehicles, Figure 1) the extents and areas of residual crush on the two vehicles provide a basis for estimating the relative velocity at impact of the vehicles. The following simplified linear analysis provides relationships for such estimates.

In Figure 1, the symbols are defined as follows.

M_1, M_2 = Masses of Vehicles 1 and 2, lb sec^2/in.

K_1, K_2 = Linear approximations of peripheral crush stiffness of contact areas of Vehicles 1 and 2, for increasing load, lb/in.

X_1, X_2 = Displacements of centers of masses, inches.

X = Displacements of peripheral interface, inches.

In the following derivation, the time derivative of a variable is indicated by a dot over the symbol for the variable, and the subscript zero is used to indicate the initial value of a variable at zero time.

Application of Newton's Second Law to the system depicted in Figure 1 yields

$$M_1\ddot{X}_1 = -\left(\frac{K_1K_2}{K_1+K_2}\right)(X_1-X_2) \qquad [1]$$

$$M_2\ddot{X}_2 = \left(\frac{K_1K_2}{K_1+K_2}\right)(X_1-X_2) \qquad [2]$$

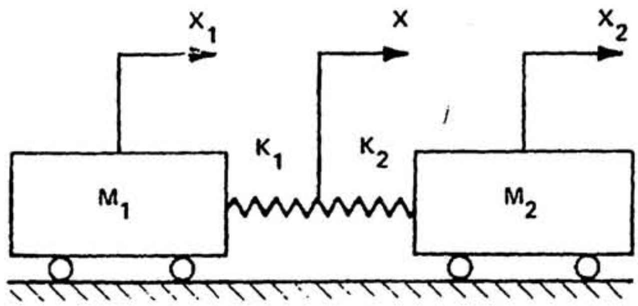

Figure 1 SCHEMATIC REPRESENTATION OF CENTRAL COLLISION

To facilitate solution of equations [1] and [2], let $\delta = X_1 - X_2$, $\dot{\delta}_0 = \dot{X}_{10} - \dot{X}_{20}$. Then equations [1] and [2] can be restated as

$$\ddot{\delta} + \left(\frac{K_1K_2}{K_1+K_2}\right)\left(\frac{M_1+M_2}{M_1M_2}\right)\delta = 0 \qquad [3]$$

Solving [3] for the maximum relative displacement,

$$(\delta)_{max} = (\dot{X}_{10} - \dot{X}_{20})\sqrt{\frac{(K_1+K_2)\ M_1M_2}{K_1K_2\ (M_1+M_2)}} \text{ inches} \qquad [4]$$

Let $\delta_1 = X_1 - X$, $\delta_2 = X - X_2$. For force equilibrium,

$$K_1\delta_1 = K_2\delta_2 \text{ lbs} \qquad [5]$$

and, by definition

$$\delta_1 + \delta_2 = \delta \text{ inches} \qquad [6]$$

Solution of [5] and [6] for δ_1 yields

$$\delta_1 = \left(\frac{K_2}{K_1+K_2}\right)\delta \quad \text{inches} \qquad [7]$$

Equation [4] can be restated in the following form,

$$\dot{X}_{10} - \dot{X}_{20} = \sqrt{\frac{(M_1+M_2)\ K_1K_2(\delta)^2_{max}}{M_1M_2\ (K_1+K_2)}} \quad \text{in/sec} \qquad [8]$$

From [7], [6] and [5],

$$\dot{X}_{10}-\dot{X}_{20} = \sqrt{\frac{(M_1+M_2)(K_1\delta_1{}^2+K_2\delta_2{}^2)}{M_1M_2}} \text{ in/sec} \qquad [9]$$

The energy absorbed in peripheral crush of Vehicles 1 and 2 can be expressed as

$$E_1 = \frac{1}{2} K_1\delta_1{}^2 \text{ lb in} \qquad [10]$$

$$E_2 = \frac{1}{2} K_2\delta_2{}^2 \text{ lb in} \qquad [11]$$

Substitution of [10] and [11] into [9] yields

$$\dot{X}_{10}-\dot{X}_{20} = \sqrt{\frac{(M_1+M_2)\ 2\ (E_1+E_2)}{M_1M_2}} \text{ in/sec} \qquad [12]$$

From Conservation of Momentum, the common velocity, V_c, may be obtained.

$$V_c = \frac{M_1\dot{X}_{10}+M_2\dot{X}_{20}}{M_1+M_2} \quad \text{in/sec} \qquad [13]$$

The velocity changes experienced by Vehicles 1 and 2 during the approach period of the collision are

$$\Delta V_1 = \dot{X}_{10}-V_c = \left(\frac{M_2}{M_1+M_2}\right)(\dot{X}_{10}-\dot{X}_{20}) \text{ in/sec} \qquad [14]$$

$$\Delta V_2 = V_c-\dot{X}_{20} = \left(\frac{M_1}{M_1+M_2}\right)(\dot{X}_{10}-\dot{X}_{20}) \text{ in/sec} \qquad [15]$$

From [14], [15] and [12], these velocity changes (approach period) can be expressed as

$$\Delta V_1 = \sqrt{\frac{2(E_1+E_2)}{M_1\ (1+{}^{M_1}/_{M_2})}}\ \text{in/sec} \tag{16}$$

$$\Delta V_2 = \sqrt{\frac{2(E_1+E_2)}{M_2\ (1+{}^{M_2}/_{M_1})}}\ \text{in/sec}\ , \tag{17}$$

Non-Central Collisions

In the more general case of non-central collisions, a common velocity is achieved at the regions of collision contact rather than at the centers of gravity. For example, in the offset frontal collision depicted in Figure 2, a common velocity is reached at point P.

In Figure 2, the collision force acting on Vehicle 1,

$$F_x = -M_1\ddot{X}_1 = -M_1\ (\ddot{X}_p - h_1\ddot{\psi}_1) \tag{18}$$

The corresponding moment acting on Vehicle 1,

$$F_x h_1 = -I_1\ddot{\psi}_1 = -M_1 k_1^{\,2}\ddot{\psi}_1 \tag{19}$$

where $k_1^{\,2}$ = radius of gyration squared of Vehicle 1 in yaw, in^2.

From [19], the angular acceleration of Vehicle 1,

$$\ddot{\psi}_1 = -\frac{F_x h_1}{M_1 k_1^{\,2}} \tag{20}$$

Substitution of [20] in [18] yields

$$\ddot{X}_p = -\frac{F_x}{M_1}\left(\frac{k_1^2+h_1^2}{k_1^2}\right) \qquad [21]$$

$$\ddot{X}_1 = -\frac{F_x}{M_1} = \left(\frac{k_1^2}{k_1^2+h_1^2}\right)\ddot{X}_p \qquad [22]$$

Let $\gamma_1 = \dfrac{k_1^2}{k_1^2+h_1^2}$, then from [22],

$$\ddot{X}_1 = \gamma_1 \ddot{X}_p \qquad [23]$$

Integration of equation [23] over the time interval during which a common velocity is reached at point P yields

$$\Delta\dot{X}_1 = \gamma_1 \Delta\dot{X}_p, \text{ or} \qquad [24]$$

$$\Delta V_1 = \gamma_1 \Delta V_1' \qquad [25]$$

where $\Delta V_1'$ is the velocity change during the approach period of the collision at point P.

From [21], the effective mass of Vehicle 1 acting at point P may be expressed as $\gamma_1 M_1$. Similarly, the effective mass of Vehicle 2 acting at point P may be expressed as $\gamma_2 M_2$. Substitution of the effective masses into equations [16] and [17] yields expressions for the velocity changes (approach period) at point P.

$$\Delta V_1' = \sqrt{\frac{2(E_1+E_2)}{\gamma_1 M_1 (1+\gamma_1 M_1/\gamma_2 M_2)}} \quad \text{in/sec} \qquad [26]$$

$$\Delta V_2' = \sqrt{\frac{2(E_1+E_2)}{\gamma_2 M_2 (1+\gamma_2 M_2/\gamma_1 M_1)}} \quad \text{in/sec} \qquad [27]$$

From equation [25] and the corresponding expression for Vehicle 2, the velocity changes (approach period) at the center of gravity of the two vehicles are obtained.

$$\Delta V_1 = \sqrt{\frac{2\gamma_1(E_1+E_2)}{M_1 (1+\gamma_1 M_1/\gamma_2 M_2)}} \qquad [28]$$

$$\Delta V_2 = \sqrt{\frac{2\gamma_2(E_1+E_2)}{M_2 (1+\gamma_2 M_2/\gamma_1 M_1)}} \qquad [29]$$

It should be noted that when $\gamma_1 = \gamma_2 = 1.00$, equations [28] and [29] reduce to the central-impact relationships of equations [16] and [17].

In Figure 3, further relationships required to approximate the effects of intervehicle friction are depicted. The effect of intervehicle friction on the direction of the resultant collision force is also given. The dimensions h_1 and h_2 are approximated on the basis of (1) the midpoint of the collision contact region, (2) the existence of a tangential velocity (columns 1 and 2 of the VDI), and (3) the intervehicle friction coefficient, μV.

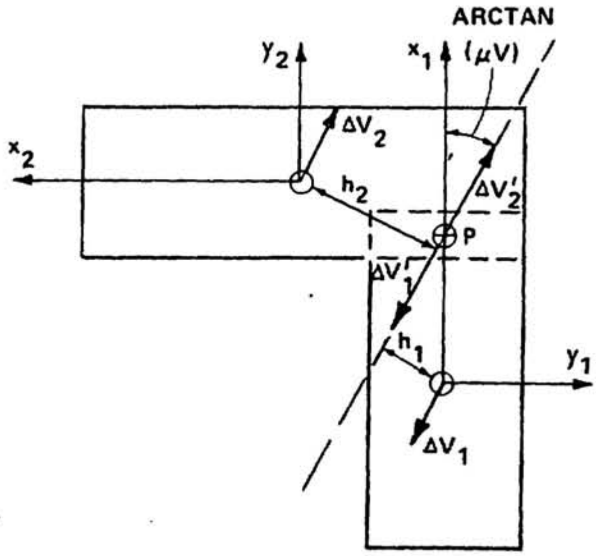

Figure 3 INTERSECTION COLLISION

In the cited study by Emori (12) and in the SMAC program (2) a simple friction coefficient has been shown to yield reasonable approximations of collision responses. Inherent in the present analytical treatment is the assumption that the residual crush provides a direct measure of the energy absorbed by compressive forces between the two vehicles and that the additional work done by tangential shear forces does not provide directly measurable damage evidence. It should be noted that the front end of the impacting vehicle in an intersection collision is generally distorted laterally, but that corresponding measurement techniques have not been established.

Absorbed Energy

The calculation of absorbed energy is based on residual crush and is patterned after that developed by Campbell (9). The only significant difference is in the treatment herein of the energy absorbed without residual crush as being proportional to the contact width rather than a constant. The following relationship is applied.

$$E_i = \int_0^{W_0} (A_i C + \frac{B_i C^2}{2} + G_i)\, dw \quad \text{in lbs} \qquad [30]$$

where E_i = Energy absorbed by vehicle i, inch lbs.

$C = f(w)$ = Residual crush of vehicle i, inches.

w = Width dimension of damaged region, inches.

A_i, B_i, G_i = Empirical coefficients of unit width properties obtained from crash test data.

Values for A_i, B_i and G_i, corresponding to the energy absorbed in barrier crashes with "standard" test weights, are stored in a table that is categorized for four vehicle sizes and for the front, side and rear of each vehicle size (Table 10). It should be noted that the frontal values in Table 10

TABLE 2-1

SUMMARY OF CRASH RESULTS

Test No.		Vehicle Size	Measured Values		Crash Values		
			Impact Speed	ΔV	Impact Speed	ΔV_1	ΔV_2
1	60° Front-to-Side	I	19.8	12.2	20.6	9.6	18.5
		S	19.8	15.6	20.4	14.4	27.7
2	60° Front-to-Side	I	31.~~5~~8	19.6	29.6	20.6	19.3
		SC	31.~~5~~8	--	33.3	30.9	29.0
6	60° Front-to-Side	I	21.5	9.2	24.9	12.4	12.7
		SC	21.~~5~~4	11.9	20.5	20.4	20.9
7	60° Front-to-Side	I	29.1	12.0	26.2	11.6	16.3
		S	29.1	16.5	27.1	25.3	35.5
8	90° Front-to-Side	I	20.~~75~~3	15.3	19.5	10.3	10.0
		I	20.~~75~~5	10.7	24.5	9.5	9.5
9	90° Front-to-Side	M	21.~~2~~	21.4	23.2	24.2	19.1
		I	21.~~2~~	8.9	22.0	11.2	8.8
10	90° Front-to-Side	M	33.3	35.1	32.7	33.6	22.4
		I	33.3	14.1	31.5	15.9	10.9
11	10° Offset Front-to-Front	S	20.4	24.0	17.2	21.0	21.1
		I	20.4	15.7	18.0	13.2	13.2
12	10° Offset Front-to-Front	S	31.5	40.1	19.8	28.2	28.2
		I	31.5	26.4	30.2	20.0	19.6
3	10° Offset Front-to-Rear	I	21.2	9.5	15.2	3.1	3.1
		S	0.0	15.8	10.4	5.4	4.9
4	10° Offset Front-to-Rear	I	38.7	18.7	31.9	10.3	9.1
		S	0.0	22.2	4.9	13.0	14.1
5	10° Offset Front-to-Rear	I	39.~~7~~3	16.3	33.8	8.1	8.1
		M	0.0	25.1	10.5	15.2	14.8

Table 10

DAMAGE DATA ,

Coeff. for Equation (30)		SUB COMPACT	COMPACT	INTER-MEDIATE	FULL SIZE	UNITS
		1.	2.	3.	4.	
COL. 3 = F	A	130.5	154.6	281.8	307.5	LB/INCH
	B	58.72	69.57	33.82	36.89	$LB/INCH^2$
	G	144.94	171.78	1174.3	1281.1	LB
COL. 3 = R, L	A	82.21	111.8	43.72	49.19	LB/INCH
	B	42.76	58.16	47.23	53.13	$LB/INCH^2$
	G	79.04	107.5	20.24	22.77	LB
COL. 3 = B	A	65.98	78.18	85.51	93.28	LB/INCH
	B	13.20	15.64	17.11	18.66	$LB/INCH^2$
	G	164.97	195.45	213.78	233.21	LB

are based on Campbell's data but that the side and rear data are gross approximations only, that are based on fragmentary crash test data. Actual vehicle weights are used in the solution of equations [28] and [29].

The developed calculation procedure permits a four-point definition of the damage profile. By default, four-point definitions are generated on the basis of column 7 of the VDI and on three "representative" types of damage profiles. The integration of equation [30] is based on trapezoidal approximations of the damage region, yielding the following equation.

$$E_i = \frac{L_i}{3} \left[\frac{A_i}{2} \quad (C_{i1}+2C_{i2}+2C_{i3}+C_{i4}) \right.$$
$$+ \frac{B_i}{6} \quad (C_{i1}^2+2C_{i2}^2+2C_{i3}^2+C_{i4}^2+C_{i1}C_{i2}+C_{i2}C_{i3}+C_{i3}C_{i4})$$
$$\left. +3\ G_i \right] \quad \text{inch lbs} \qquad [31]$$

The "equivalent barrier speed" as defined by Campbell (9) is not equal to the speed change, ΔV, in low speed collisions, since the rebound velocity produced by the coefficient of restitution is not included. At the velocity intercept of the linearized fit of impact velocity plotted against residual crush, elastic behavior is indicated for the vehicle crush. The total speed change, ΔV, should, therefore, be equal to twice the impact velocity in that velocity range, in the absence of an energy absorbing bumper device.

The impact speeds without residual crush that are indicated by Campbell's linear fits (no actual data points at impact speeds below 15 MPH) suggest substantially higher coefficients of restitution than, for example, the values presented by Emori in (12). Without more definitive information on the actual magnitude and variation of the coefficient of restitution as a function of both deflection extent and position on the vehicle periphery, the complexity of introducing a corresponding refinement in the damage analysis technique cannot be justified. Therefore, the damage analysis procedure defined herein tends to underestimate ΔV in low speed collisions.

SPINOUT ANALYSIS

In (8), Marquard defines relationships for approximating the initial linear and angular (yaw) velocities of a vehicle in a spinout trajectory (i.e., at the point of separation subsequent to a collision) on the basis of the energy dissipated during its changes in position and orientation between separation and rest. He includes the cases of freely rotating wheels and of locked wheels, each with the front wheels limited to the straight ahead position of steering.

In the case of freely rotating wheels, the linear and angular velocities of the vehicle are decelerated alternately as the heading direction changes with respect to the direction of the linear velocity. When the vehicle slides laterally, the side forces at the front and rear tires tend to have the same direction despite the existence of a yaw velocity. Therefore, during this phase of the motion, the angular velocity tends to remain constant while the linear velocity is decelerated. When the longitudinal axis is aligned with the direction of the linear velocity, the side forces at the front and rear tires act in opposite directions and the angular velocity is decelerated while the linear velocity tends to remain constant. A SMAC-generated example of the time-histories of angular and linear velocity, for the case of no braking, is shown in Figure 4. Marquard defines a different form of solution for the case of locked wheels, whereby the ratio of angular to linear displacement during the spinout is used to determine empirical coefficients.

The derivation of equations in (8) is not completely presented. Therefore, some details of the assumptions must be deduced from the final form of the equations.

In the following outline of the derivation, the time derivative of a variable is indicated by a dot over the symbol for the variable and the subscript S is used to indicate the value of a variable at the point of separation.

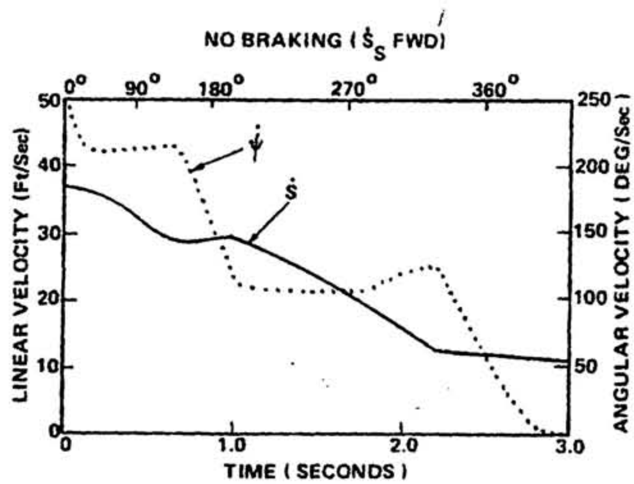

Figure 4 LINEAR AND ANGULAR VELOCITY VS TIME

Spinout Without Braking

In Figure 5, an idealized plot of the time histories of linear and angular velocities is depicted. The symbols T_1 and T_2 are used to represent the times, subsequent to separation, at which the linear and angular velocities, respectively, reach zero values. The areas under the velocity plots are, of course, equal to the corresponding linear and angular displacements. If it is assumed that reasonable approximations of the areas under the two velocity plots can be obtained from the triangles shown in Figure 5 as broken lines, the following relationships can be applied.

$$\Delta\psi \cong \left(\frac{\dot{\psi}_s}{2}\right) T_1, \text{ and} \tag{32}$$

$$S \cong \left(\frac{\dot{S}_s}{2}\right) T_2 \tag{33}$$

During the periods of angular deceleration, the magnitude of that deceleration can be approximated as

$$\ddot{\psi} \cong \frac{\mu g}{k^2} \left(\frac{a+b}{2}\right) \tag{34}$$

where μ = nominal tire-ground friction coefficient.

g = acceleration of gravity, in/sec^2.

k^2 = radius of gyration squared for complete vehicle in yaw, in^2.

$(a+b)$ = wheelbase, inches.

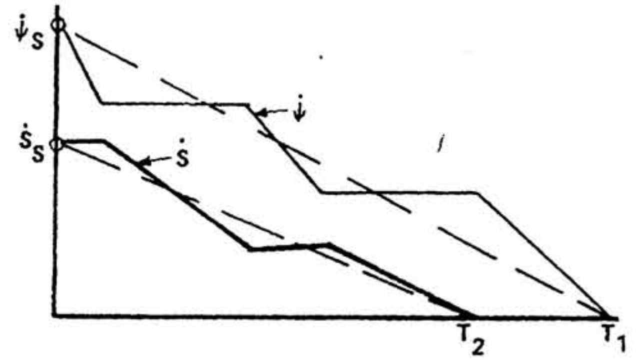

Figure 5 IDEALIZED PLOT OF VELOCITIES VS TIME

From equation [34] the actual deceleration time of the angular velocity can be approximated as

$$t_1 = \frac{\dot{\psi}_s}{\ddot{\psi}} = \frac{2\dot{\psi}_s k^2}{\mu g(a+b)} \qquad [35]$$

During the linear deceleration portion of the motion (i.e., for orientations near that of broadside sliding), the tire side forces, which are perpendicular to the wheel planes, act at a changing angle with respect to the direction of the linear velocity. If the average value of the cosine of the angle during that portion of the motion is taken to be 0.85, the average magnitude of the linear deceleration during periods of linear deceleration can be approximated as

$$\ddot{S} \cong 0.85\ \mu g \qquad [36]$$

The corresponding actual deceleration time of the linear velocity can be approximated by

$$t_2 = \frac{\dot{S}_s}{\ddot{S}} = \frac{\dot{S}_s}{0.85\ \mu g} \qquad [37]$$

The total time required to stop both the linear and the angular motions can be expressed, from equations [35] and [37] as

$$T = t_1 + t_2 = \frac{2\dot{\psi}_s k^2}{\mu g(a+b)} + \frac{\dot{S}_s}{0.85\ \mu g} \qquad [38]$$

If it is assumed that both phases of the motion end at approximately the same time,

$T \approx T_1 \approx T_2$, then from [32] and [33],

$$\frac{2(\Delta\psi)}{\dot{\psi}_s} \approx \frac{2S}{\dot{S}_s} \approx T \qquad [39]$$

From [39],

$$\frac{\dot{S}_s}{\dot{\psi}_s} \approx \frac{S}{\Delta\psi} \qquad [40]$$

Substitution of [39] and [40] into [38] yields

$$\frac{2(\Delta\psi)}{\dot{\psi}_s^{\,2}} = \frac{2k^2}{(a+b)\ \mu g} + \frac{S}{0.85\ \mu g \Delta\psi} \qquad [41]$$

Solution of [41] for $\dot{\psi}_s$ yields

$$\dot{\psi}_s = \sqrt{\frac{\mu g(\Delta\psi)^2}{\frac{k^2}{(a+b)}\ \left|\Delta\psi\right| + \frac{S}{1.70}}}\ \mathrm{sgn}\ (\Delta\psi) \qquad [42]$$

From [38] and [39],

$$\dot{S}_s = 1.70 \left[\frac{\mu g(\Delta\psi)}{\dot{\psi}_s} - \frac{k^2|\dot{\psi}_s|}{(a+b)} \right] \qquad [43]$$

Equations [42] and [43] correspond to the relationships defined by Marquard in (8). The relationships defined by [42] and [43] were extended to include the case of partial braking, in the following manner.

If θ is used to define the decimal portion of full deceleration produced by braking or wheel damage, where $0 \leq \theta \leq 1.00$, a linear deceleration of $0.85\ \theta\mu g$ occurs during t_1, the deceleration time of the angular velocity. Therefore, the linear velocity to be decelerated in the corresponding phase of motion is reduced to

$$\dot{S}_1 = \dot{S}_s - 0.85\ \theta\mu g t_1 \qquad [44]$$

The total time required for linear deceleration is reduced to

$$t_2 = \frac{\dot{S}_1}{0.85\ \mu g} = \frac{\dot{S}_s}{0.85\ \mu g} - \theta t_1 \qquad [45]$$

Therefore, the total time required to stop both the linear and the angular motions becomes

$$T = t_1 + t_2 = \frac{\dot{S}_s}{0.85\mu g} + (1-\theta)\ \frac{2\dot{\psi}_s k^2}{(a+b)\mu g} \qquad [46]$$

With the introduction of θ, equations [42] and [43] become

$$\dot{\psi}_s = \sqrt{\frac{\mu g\ (\Delta\psi)^2}{\left(\frac{k^2}{a+b}\right)\ |\Delta\psi|\ (1-\theta) + \frac{S}{1.70}}}\ \mathrm{sgn}\ \Delta\psi \qquad [47]$$

$$\dot{S}_s = 1.70\left[\frac{\mu g\ (\Delta\psi)}{\dot{\psi}_s} - \frac{k^2\ |\dot{\psi}_s|\ (1-\theta)}{(a+b)}\right] \qquad [48]$$

Application of equations [47] and [48] to a number of SMAC-generated spinout trajectories revealed several shortcomings. First, it was found that a residual linear velocity frequently exists at the end of the rotational motion. Thus, equations [39] and [40] can introduce large errors. Next it was found that the shapes of the plots of linear and angular velocity vs. time change substantially as functions of the initial ratio of linear to angular velocity, affecting the accuracy of simple linear approximations of the areas under the curves. Finally, the transitions between the different deceleration rates in the linear and angular motions do not occur abruptly. Rather, slope changes in the plots of velocities against time occur gradually, producing rounded "corners" in the curves (e.g., see Figure 4). As a result of the transitions, the effective deceleration rates in the two modes of motion are somewhat smaller than those corresponding to the full value of tire-ground friction.

To improve the accuracy of the approximations, provision was made for introduction of a residual linear velocity at the end of the rotational motion and empirical coefficients, in the form of polynomial functions of the initial ratio of linear to angular velocity. Since that velocity ratio is initially unknown, a solution procedure was developed whereby several trial values of the ratio, based on an approximate equation, are used to obtain multiple solutions. The solution for which the velocity ratio most closely matches the corresponding trial value is retained. The residual linear velocity is approximated on the basis of the distance traveled subsequent to the end of the rotational motion. The corresponding derivation of equations is outlined in the following.

The total time required to stop the angular motion is approximated by

$$T_1 = \alpha_1 \frac{\Delta\psi}{\dot{\psi}_s} = t_1 + t_2 \qquad [49]$$

The actual time of angular deceleration,

$$t_1 = \frac{2\dot{\psi}_s k^2}{(a+b)\mu g \alpha_2} \quad [50]$$

The actual time during which linear acceleration occurs,

$$t_2 = \frac{(\dot{S}_s - \dot{S}_1)}{\alpha_4 \mu g} - \frac{\alpha_3 \theta t_1}{\alpha_4} \quad [51]$$

The change in linear velocity during time T_1, can be approximated as

$$S_1 = \left(\frac{\dot{S}_s + \dot{S}_1}{\alpha_5}\right) T_1 \quad [52]$$

From [49] and [52]

$$\alpha_1 \frac{\Delta\psi}{\dot{\psi}_s} = \alpha_5 \frac{S_1}{(\dot{S}_s + \dot{S}_1)} \quad [53]$$

From [49], [50] and [51],

$$\alpha_1 \frac{\Delta\psi}{\dot{\psi}_s} = \frac{2\dot{\psi}_s k^2}{(a+b)\mu g \alpha_2}\left(1 - \frac{\alpha_3 \theta}{\alpha_4}\right) + \frac{\dot{S}_s - \dot{S}_1}{\alpha_4 \mu g} \quad [54]$$

From [53],

$$(\dot{S}_s - \dot{S}_1) = \frac{\alpha_5}{\alpha_1} \frac{S_1 \dot{\psi}_s}{\Delta\psi} - 2\dot{S}_1 \quad [55]$$

Substituting [55] in [54],

$$\dot{\psi}_s^2 + B\,\dot{\psi}_s + C = 0 \qquad [56]$$

where

$$B = \frac{\dot{S}_1\,|\Delta\psi|}{D} \qquad [57]$$

$$C = \frac{\alpha_1\alpha_4\mu g(\Delta\psi)^2}{2D} \qquad [58]$$

$$D = \frac{\alpha_4 k^2\,|\Delta\psi|\,(1-\frac{\alpha_3\theta}{\alpha_4})}{\alpha_2(a+b)} + \frac{\alpha_5 S_1}{2\alpha_1} \qquad [59]$$

From [54]

$$\dot{S}_s = \dot{S}_1 + 2\alpha_4 \left\{ \frac{\alpha_1\mu g\Delta\psi}{2\dot{\psi}_s} - \frac{\dot{\psi}_s k^2\left(1-\frac{\alpha_3\theta}{\alpha_4}\right)}{(a+b)\alpha_2} \right\} \qquad [60]$$

The detailed solution procedure for equations [56] through [60] is outlined in Appendix 1. It should be noted that the developed equations reduce to the form of [47] and [48] when the residual linear velocity is set to zero and the coefficients, α_i, are set to constant values. Also, the developed relationships apply to the case of fully locked wheels as well as rotating wheels, eliminating the need for a separate "locked wheel" procedure such as that defined in (8).

CONCLUDING REMARKS

The described closed-form calculation procedure of the CRASH program has been shown to be capable of yielding impact velocity approximations with a $\pm$ 12% accuracy. The operating cost ranges from only \$1.00 to \$5.00 per case, depending on the extent of the available case data. Thus, the CRASH program, by itself, is considered to be a valuable aid to accident investigation in cases (1) where the evidence is not sufficiently complete to justify the larger costs of the SMAC program or (2) where large numbers of existing accident reports are to be processed to obtain uniformly derived, low-cost estimates of impact velocities and velocity changes. The availability of the SMAC computer program to generate detailed collision response data has been highly beneficial to the described development.

APPENDIX 1

Subroutine SPIN II

Inputs:

X'_{c1}, Y'_{c1}, ψ_1 = Position and orientation at end of rotation (feet and degrees).

X'_{cs}, Y'_{cs}, ψ_s = Position and orientation at separation (feet and degrees).

$\dot{S}_1$ = Residual linear velocity at end of rotation (ft/sec).

$a+b$ = Wheelbase, inches.

k^2 = Radius of gyration squared for complete vehicle in yaw, in^2.

μ = Nominal tire-ground friction coefficient.

θ = Decimal portion of full deceleration, $0 \leq \theta \leq 1.000$.

g = Acceleration of gravity

= 386.4 inches/sec^2.

1. $S_1 = 12\sqrt{(X'_{c1}-X'_{cs})^2+(Y'_{c1}-Y'_{c2})^2}$ inches

2. $\Delta\psi = \dfrac{(\psi_1-\psi_s)}{57.3}$ radians

3. $$\gamma_s = \arctan\left(\frac{Y'_{cl}-Y'_{cs}}{X'_{cl}-X'_{cs}}\right)$$

4. For $\theta = 1.0$,

$$\rho' = 1.408\left(\frac{S_1}{|\Delta\psi|} - 32\right)$$

For $\theta < 1.0$,

$$\rho' = \frac{-b + \sqrt{b^2-4ac}}{2a}$$

where $a = (1-\theta)\ 8.52\text{x}10^{-4}$

$b = 0.94-0.23\theta$

$c = 40.64-8.64\theta - \frac{S_1}{|\Delta\psi|}$

5. $\rho_1 = 0.70\rho'$

$\rho_2 = 0.85\rho'$

$\rho_3 = \rho'$

$\rho_4 = 1.15\rho'$

$\rho_5 = 1.30\rho'$

6. For each ρ_j, calculate α_{ij}, where

$i = 1,2,3,4,5$

$j = 1,2,3,4,5$

For $0 \leq \rho_j \leq 250$,

$$\alpha_{ij} = a_{i0}+a_{i1}\rho_j+a_{i2}\rho_j^2+a_{i3}\rho_j^3$$

For $250 < \rho_j$,

$$\alpha_{ij} = K_i$$

where

	i				
	1	2	3	4	5
a_o	2.58	0.88	0.2417	0.671	1.223
a_1	-7.44×10^{-3}	-3.92×10^{-3}	4.85×10^{-3}	1.4772×10^{-3}	1.7307×10^{-2}
a_2	1.504×10^{-5}	8.0×10^{-6}	-9.667×10^{-6}	-4.50×10^{-6}	-1.053×10^{-4}
a_3	0	0	0	5.80×10^{-9}	1.993×10^{-7}
K	1.66	0.400	0.850	0.850	2.08

7. $$D_j = \left\{ \frac{\alpha_{4j} k^2 |\Delta\psi| \left(1 - \frac{\alpha_{3j}\theta}{\alpha_{4j}}\right)}{\alpha_{2j}(a+b)} + \frac{\alpha_{5j} S_1}{2\alpha_{1j}} \right\}$$

8. $$B_j = \frac{12\dot{S}_1 |\Delta\psi|}{D_j}$$

9. $$C_j = \frac{\alpha_{1j}\alpha_{4j}\mu g(\Delta\psi)^2}{2D_j}$$

10. $$\dot{\psi}_{sj} = \left\{ \frac{B_j}{2} + \frac{1}{2}\sqrt{B^2_j + 4C_j} \right\} \text{sgn } (\Delta\psi) \text{ rad/sec}$$

11. $$\dot{S}_{sj} = 12\dot{S}_1 + 2\alpha_{4j} \left\{ \frac{\alpha_{1j}\mu g(\Delta\psi)}{2\dot{\psi}_{sj}} - \frac{|\dot{\psi}_{sj}| k^2 \left(1 - \frac{\alpha_{3j}\theta}{\alpha_{4j}}\right)}{(a+b)\alpha_{2j}} \right\} \text{ inches/sec}$$

12. $$\beta_j = \frac{\rho_j |\dot{\psi}_{sj}|}{\dot{S}_{sj}} - 1$$

Let n = the value of j for which $|\beta_j|$ is smallest.

13. $\dot{\psi}_s = 57.3\ \dot{\psi}_{sn}$ degrees/sec

14. $\dot{S}_s = \dot{S}_{sn}$ inches/sec

15. $U_s = \dot{S}_s \cos(\gamma_s - \psi_s)$ inches/sec

16. $V_s = \dot{S}_s \sin(\gamma_s - \psi_s)$ inches/sec

17. Return with starting values:

U_s inches/sec

V_s degrees/sec

$\dot{\psi}_s$ degrees/sec

ACKNOWLEDGMENTS

The author wishes to acknowledge contributions of Mr. James P. Lynch to development of the format and coding of the CRASH computer program. Also, the work of Dr. Ian S. Jones and Mrs. Camille F. Bainbridge on START, which was developed as a "starting routine" for the SMAC program and was the predecessor to CRASH, contributed directly to the success of the present research.

REFERENCES

1. McHenry, R. R., "Development of a Computer Program to Aid the Investigation of Highway Accidents," Calspan Report No. VJ-2979-V-1, December 1971 (PB #208537, Contract No. FH-11-7526).

2. McHenry, R. R., Segal, D. J., Lynch, J. P., and Henderson, P. M., "Mathematical Reconstruction of Highway Accidents," Calspan Report No. ZM-5096-V-1, January 1973 (PB #220150, Contract No. DOT-HS-053-1-146).

3. Bartz, J. A., Segal, D. J., and McHenry, R. R., "Mathematical Reconstruction of Accidents - Analytical and Physical Reconstruction of Ten Selected Highway Accidents," Calspan Report No. ZQ-5341-V-1, March 1974 (Contract No. DOT-HS-053-3-658).

4. McHenry, R. R., "A Computer Program for Reconstruction of Highway Accidents," paper presented at the 17th Stapp Car Crash Conference, November 12-13, 1973.

5. Jones, I. S. and Segal, D. J., "The Application of the SMAC Accident Reconstruction Program to Actual Highway Accidents," paper presented to the American Association for Automotive Medicine, 13 September 1974.

6. Jones, I. S., "Results of Selected Applications to Actual Highway Accidents of the SMAC Reconstruction Program," paper presented at the 18th Stapp Car Crash Conference, December 1974.

7. McHenry, R. R., Jones, I. S., and Lynch, J. P., "Mathematical Reconstruction of Highway Accidents - Scene Measurement and Data Processing System," Calspan Report No. ZQ-5341-V-2, December 1974 (Contract No. DOT-HS-053-3-658).

8. Marquard, E., "Progress in the Calculations of Vehicle Collisions," Automobiltechnische Zeitschrift, Jahrq. 68, Heft 3, 1966, pp. 74-80.

9. Campbell, K. L., "Energy Basis for Collision Severity," SAE Paper No. 740565, Proceedings of the 3rd International Conference on Occupant Protection, Troy, Michigan, July 10-12, 1974.

10. "Collision Deformation Classification," Society of Automotive Engineers Technical Report J224a, 1972.

11. Emori, R. I., "Analytical Approach to Automobile Collisions," SAE Paper No. 680016, Automotive Engineering Congress, Detroit, Michigan, January 8-12, 1968.

12. Emori, R. I., "Mechanics of Automobile Collisions," First International Conference on Vehicle Mechanics," Wayne State University, Detroit, Michigan, July 16-18, 1968.

13. Severy, D. M., Mathewson, J. H., and Siegel, A. W., "Automobile Side-Impact Collisions, Series II," SAE SP-232.

14. DeLeys, N. J., Segal, D. J., and Patten, J. S., "Underride/Override of Automobile Front Structures in Intervehicular Collisions," Volume 2 "Car-to-Car Head-On Impacts," Calspan Report No. VJ-2844-V-3, December 1971.

15. Bartz, J. A. and Butler, F. E., "A Three-Dimensional Computer Simulation of a Motor Vehicle Crash Victim - Phase 2 - Validation Study of the Model," Calspan Report No. VJ-2978-V-2, December 1972.

16. Greene, J. E., "Basic Research in Crashworthiness II - Side Impact Tests of Unmodified Vehicles," Calspan Report No. YB-2987-V-9, February 1973.